Theory of laser wakes in plasma channels

G. Shvets and X. Li
Princeton Plasma Physics Laboratory, Princeton, New Jersey 08543

(Received 21 July 1998; accepted 21 October 1998)

Excitation of accelerating modes in transversely inhomogeneous plasma channels is considered as an initial value problem. Discrete eigenmodes are supported by plasma channels with sharp density gradients. These eigenmodes are collisionlessly damped as the gradients are smoothed. Using collisionless Landau damping as the analogy, the existence and damping of these ''quasi-modes'' is studied by constructing and analytically continuing the causal Green's function of wake excitation into the lower half of the complex frequency plane. Electromagnetic nature of the plasma wakes in the channel makes their excitation nonlocal. This results in the algebraic decay of the fields with time due to phase-mixing of plasma oscillations with spatially-varying frequencies. Characteristic decay rate is given by the mixing time τ_m, which corresponds to the dephasing of two plasma fluid elements separated by the collisionless skin depth. For wide channels analytic expressions for the field evolution are derived. Implications for electron acceleration in plasma channels are discussed. © *1999 American Institute of Physics.* [S1070-664X(99)00902-7]

I. INTRODUCTION

Plasma channel is an important tool for a variety of laser-plasma applications, such as laser-driven particle accelerators,[1–8] x-ray lasers,[9,10] harmonic generation,[11] and inertial confinement fusion.[12] The primary objective of creating a plasma channel is to guide radiation (e.g., an intense laser pulse in a laser wakefield accelerator) over many Rayleigh lengths. Underdense plasma channels can support transversely localized laser modes which do not diffract. Since the frequencies of such modes are typically much higher than plasma frequencies anywhere in the channel, these eigenmodes are almost purely electromagnetic. Laser guiding in plasma channels has been studied theoretically and experimentally.[13,14]

Inhomogeneous plasma channels support another class of the lower frequency modes, which have both the electrostatic and electromagnetic characteristics. These modes are the extensions of electrostatic modes of the cold uniform plasma of density n_0, which have the plasma frequency $\omega_p = (4\pi e^2 n_0/m)^{1/2}$, where $-e$ and m are the electron charge and mass, respectively. Waves in inhomogeneous plasmas have been studied since the 1960's because of their relevance to the resonant absorption of obliquely incident p polarized radiation.[15–17] Calculations of the rate of energy absorption assume a cw incident electromagnetic wave of fixed-frequency ω_0, resonantly driving a cold plasma wave in the close proximity of the plasma resonance point x_r, defined by $\omega_p(x_r)=\omega_0$. Electromagnetic surface modes of the semi-infinite plasma were first studied by Stepanov,[18] who pointed out that these surface modes become damped as the sharp plasma-vacuum interface is smoothed out. Excitation of the *electrostatic* waves in inhomogeneous plasmas was studied as an initial value problem by Sedláček.[19] However, the electrostatic assumption does not hold in general.

Applications of plasma waves to particle acceleration brought about the renewed interest in the accelerating wakes in plasma channels.[20–25] It was demonstrated[20,21] that the accelerating properties of the surface wave, generated in a hollow plasma channel, are superior to those of the electrostatic wake in a homogeneous plasma. In particular, the wake is transversely homogeneous inside the channel, and the magnetic component of the wake, combined with the radial electric field, prevents the over-focusing of the accelerated particles.[24] Excitation of the accelerating wakes in an arbitrary plasma channel by a short intense laser pulse was first considered by Shvets *et al.*,[22,23] with the emphasis on the hollow channels with a sharp (although not infinitely sharp) plasma-vacuum interface.

One of the interesting features of wake excitation in plasma channels with sharp density gradients is the excitation of a damped quasi-mode. This quasi-mode, whose frequency is very close to the frequency of the surface mode in a hollow channel, resonates with the plasma at the resonant location x_r, defined by $\omega_p(x_r)=\omega_{\rm ch}$, where $\omega_{\rm ch}=\omega_{p0}/\sqrt{1+\omega_{p0}b/c}$ is the frequency of the surface wave, b is the channel width and ω_{p0} is the plasma frequency. Very large electric fields develop at x_r, eventually leading to wave breaking and plasma heating.

It turns out that the response of a plasma channel with a smooth density profile contains a continuous spectrum of frequencies, unlike the response of a hollow channel with an infinitely sharp interface, which only supports a single surface mode at $\omega_{\rm ch}$ and a bulk plasma mode at ω_{p0}. The discrete channel mode is collisionlessly damped in the presence of the continuum of modes. Dissipationless damping of quasi-modes in the presence of the mode continuum is a ubiquitous phenomenon in the physics of continuous media. The well known examples include collisionless damping of plasma waves in warm unmagnetized plasmas (Landau damping),[26] Alfven waves in ideal magnetohydrodynamics, modes of inviscid fluid motion,[27] and oscillations of strongly magnetized electron columns.[28,29]

Presently, an interesting dichotomy exists in our understanding of wake excitation in nonuniform plasmas. Two radically different plasma profiles can be treated, at least perturbatively: (i) almost uniform plasma (e.g., a shallow parabolic plasma channel of width much exceeding both the collisionless skin depth and the spot size of the ponderomotive driver[25,30,31]); (ii) plasma channel consisting of a finite number of piecewise constant density steps (e.g., a hollow channel). The purpose of this work is to present a unified theory of plasma modes in arbitrary plasma channels. This work relies heavily on the ideas of Briggs *et al.*[28] for solving the initial value problem for the inviscid fluid flows and oscillations of magnetized electron columns. Despite the differences in the equations describing the excitation of accelerating wakes in plasma channels, and those solved by Briggs *et al.*, the general concepts of causality, analytic continuation of the dispersion function and eigenfunctions into the complex frequency plane, and integrating differential equations in the complex x-plane can be applied to the problem at hand.

The remainder of the paper is organized as follows. In Sec. II the equations for wake excitation in nonuniform cold plasma by a laser pulse are reviewed. Excitation of the electromagnetic eigenmode of a hollow channel is also described. In Sec. III we show that plasma channels with smooth monotonic density profiles do not support any neutral or damped eigenmodes. Wake excitation by an arbitrary laser pulse is formally calculated in Sec. IV, where the Green's function of the wake excitation is derived and analytically continued into the lower half of the ω plane. It is shown that electric and magnetic fields can be computed by summing the contributions of several cuts and poles of the Green's function. Contributions from the cuts describe the (almost) local wake excitation, while the poles correspond to the global collisionlessly damped quasi-modes. Frequencies, damping rates, and excitation of these quasi-modes are considered in Sec. V. After several damping times, exponential decay of the fields is replaced by the power-law decay of the locally excited wakes. Long-time asymptotic analysis of these wakes is carried out in Sec. VI, where the contributions of the cuts of the Green's function are evaluated. In Sec. VII we calculate wake excitation in wide plasma channels, where the density gradient scale is much longer than c/ω_p. We find that for wide channels quasi-modes are not important. Accelerating electric field E_z and magnetic field B_y decay in time according to (different) power laws, while the focusing field E_x reaches the steady state for $t=\infty$. Power law decay is demonstrated to be the result of phase mixing of adjacent plasma fluid elements, which oscillate with their local plasma frequencies. Section VIII presents the discussion of the results.

II. THE MODEL OF WAKE EXCITATION

A number of simplifying assumptions make the problem at hand analytically tractable. Slab geometry is assumed, so that the plasma density $n_0(x)$ is only a function of the transverse coordinate x. Ions are assumed immobile, providing a neutralizing background. Wakes are driven by a nonevolving nonrelativistic laser pulse with $a=e|A|/mc^2<1$, so that all calculations are performed to order a^2. For large a, the ponderomotive force will significantly distort the plasma channel, precluding the analysis based on a prescribed density profile. The group velocity of the pulse is assumed close to c (tenuous plasma), and all the plasma quantities are functions of $\zeta=t-z/c$.

For tenuous plasma $\omega_p \ll \omega_0$ two separate time scales exist: fast scale of order the laser period, $1/\omega_0$, and slow scale of order the plasma period, $1/\omega_{p0}$. On a slow time scale, consistently with a weakly relativistic assumption, electrons are driven by the ponderomotive force of the laser and the electric field of the wake:

$$\frac{\partial \mathbf{v}}{\partial \zeta}=\frac{e}{m}(\mathbf{E}+\nabla f), \tag{1}$$

where f is the ponderomotive potential given by

$$f=-\frac{mc^2}{4e}|\mathbf{a}|^2, \tag{2}$$

and E is the electric field induced in the plasma. Assuming quiescent plasma in front of the laser pulse and Laplace transforming the electron fluid equation of motion (2) in ζ yields the electron current density $\mathbf{j}=-en_0\mathbf{v}$. The electric field of the wake is computed by substituting $\mathbf{j}$ into Ampere's law:

$$\epsilon\tilde{\mathbf{E}}=\frac{\omega_{p0}^2(x)}{\omega^2}\nabla\tilde{f}+i\frac{c}{\omega}\nabla\times\tilde{\mathbf{B}}, \tag{3}$$

where ϵ is the cold plasma dielectric function:

$$\epsilon(x,\omega)=1-\frac{\omega_{p0}^2(x)}{\omega^2}, \tag{4}$$

and the tilted variables are Laplace transforms in ζ and functions of the transform variable ω. As Eq. (3) indicates, the total electric field is a sum of the locally excited plasma perturbation (first term) and a global electromagnetic field (second term), which we denote $\boldsymbol{\mathcal{E}}$. The significance of the two contributions is determined by the channel profile. For example, in a hollow channel the contribution of the first term vanishes in the vacuum region, and the second term (electromagnetic surface mode) dominates. The second term identically vanishes in the homogeneous plasma, and becomes very small for very smooth density profiles. This is because ponderomotively excited wakes in homogeneous plasmas are electrostatic in the weakly relativistic approximation. Small magnetic field of the order $B\sim a_0^4 mc\omega_p/e$, which is generated in the homogeneous plasma,[32] is neglected in this calculation.

The equation for the magnetic field is derived by substituting Eq. (3) into Faraday's law:

$$B_y''-\frac{\epsilon'}{\epsilon}B_y'-\frac{\omega_p^2(x)}{c^2}B_y=\frac{\omega^2}{c^2}\frac{\epsilon'}{\epsilon}\tilde{f}(x,\omega). \tag{5}$$

Since we only consider accelerating TM modes, boundary conditions $\tilde{B}_y(x=0)=\tilde{B}_y(x=\infty)=0$ must be satisfied. Assuming a monotonic density plasma density profile, which asymptotes to n_0 at infinity, one can choose a transverse

location $x_{\max}$ (finite or infinite), such that $\omega_p(x)\equiv\omega_{p0}$ for $x>x_{\max}$. Therefore, the second boundary condition can be chosen at $x_{\max}$ as $\tilde{B}'+k_{p0}B=0$. Equation (5) can be recast as

$$\mathcal{L}_S(\omega)B_y=\frac{\omega^2}{c^2}\frac{\epsilon'}{\epsilon^2}\tilde{f}(x,\omega), \tag{6}$$

where $\mathcal{L}_S$ is a Sturm–Liouville operator, parametrically dependent on a (possibly complex) frequency ω:

$$\mathcal{L}_S(\omega)=\frac{d}{dx}\left(\frac{1}{\epsilon(x,\omega)}\frac{d}{dx}\right)-\frac{\omega_p^2(x)}{c^2\epsilon(x,\omega)}. \tag{7}$$

A possible approach to solving Eq. (6) is to find the normal modes of the operator $\mathcal{L}_S$. As shown below for the hollow plasma channel, such an approach is elucidating when the plasma density profile is a piecewise constant function. It is, however, problematic when applied to arbitrary density profiles. The deficiencies of the normal modes method for a conceptually similar problem of two-dimensional motions of the inviscid incompressible fluid have been known for many years, ever since this method was first applied by Rayleigh.[33] More recently, the major three problems with this method were summarized by Briggs,[28] and we follow his account here. The first problem was noted by Kelvin[34] in a paper titled ''On a disturbing infinity in Lord Rayleigh's solution for waves in a plane vortex stratum,'' which, in the context of wake excitation, refers to the resonant coupling of the electromagnetic eigenmode to the electrostatic plasma waves when its frequency matches the local plasma frequency. The second problem is that the normal modes of a piecewise constant density profile *disappear* as soon as the profile is smoothed out. The third problem is that a finite number of the normal modes cannot form a mathematically complete set.

However, the method of normal modes proved useful in analyzing the hollow plasma channel. It was shown[21] that for the plasma density profile

$$\omega_p^2(x)=\begin{cases}0 & \text{for } |x|<b\\ \omega_{p0} & \text{for } |x|>b\end{cases} \tag{8}$$

a single normal mode with frequency $\omega_{\rm ch}=\omega_{p0}/\sqrt{1+\omega_{p0}b/c}$ exists. This is a surface mode because it can be shown that the electron fluid is incompressible for $|x|>b$, while there is a surface charge at $|x|=b$. Since $0<\omega_{\rm ch}<\omega_{p0}$, it is very plausible that the normal mode may be strongly perturbed if the interface between vacuum and plasma is not infinitely sharp, i.e., there exists a location x_r where $\omega_p(x_r)=\omega_{\rm ch}$. At this location $\epsilon(x_r,\omega_{\rm ch})=0$, and the operator $\mathcal{L}_S$ becomes singular. This is the essence of the first problem with the method of normal modes applied to a general density profile. It was also shown in Refs. 22, 23 that the time evolution of the electromagnetic field inside the channel is completely determined by the excitation of a single surface mode. For example, the transversely homogeneous inside the channel accelerating field E_z is given by

$$E_z(\zeta)=\frac{\omega_{p0}^2}{(1+k_pb)c}\int_{-\infty}^{\zeta}d\zeta'\frac{\sin\omega_{\rm ch}(\zeta-\zeta')}{\omega_{\rm ch}}\frac{df(\zeta',x=b)}{d\zeta'}. \tag{9}$$

A noteworthy consequence of Eq. (9) is that the amplitude of the surface mode is driven by the *longitudinal* rather than the transverse gradient of the ponderomotive potential f. Hence, despite the significant transverse pressure, exerted by a narrow laser pulse on the plasma, the pulse still has to be short to excite a substantial wake inside the channel.

The situation dramatically changes when the transition between vacuum and plasma occurs over a finite distance $b\delta$, where δ may be arbitrarily small. A continuum of modes is required to describe the fields over a continuous (albeit short) transitional region, with each spatial location having its own local plasma frequency. This explains the third problem with the normal mode expansion, which only produces a single normal mode. In the next section, to demonstrate the second problem with the normal mode method, we show that, in fact, no neutral or damped modes exist for smooth density profiles.

III. EXISTENCE OF NORMAL MODES FOR SMOOTH DENSITY PROFILES

To study the normal modes of a plasma channel, assume that the plasma frequency varies monotonically from ω_{p1} to ω_{p2} between $x=0$ and $x=x_{\max}$. Allowing $x_{\max}$ to be finite or infinite, further assume, without loss of generality, that plasma density is constant and equal to ω_{p2} for $x>x_{\max}$. If ψ is an eigenmode of the linear operator $\mathcal{L}_S(\omega)$, where $\omega=\omega_{re}+i\omega_i$ is a complex frequency, it can be shown that $\psi(x)=Ce^{-k_p(x-x_{\max})}$ for $x>x_{\max}$. Multiplying $\mathcal{L}_S\psi=0$ by ψ^* and integrating between $x=0$ and $x=x_{\max}$ yields

$$-k_p|C|^2=\int_0^{x_{\max}}dx\frac{\omega^2-\omega_{p2}^2}{\omega^2-\omega_p^2(x)}\left(\frac{\omega_p^2(x)}{c^2}|\psi|^2+\left|\frac{d\psi}{dx}\right|^2\right). \tag{10}$$

Considering damped or growing modes with $\omega_i\neq0$, and assuming that both ψ and ψ' are continuous between 0 and $x_{\max}$, find that the imaginary part of the right-hand side (RHS) of Eq. (10) does not vanish. Since the imaginary part of the left-hand side (LHS) of Eq. (10) is equal to zero, the existence of the damped or growing eigenmodes is ruled out.

Next we check for the existence of neutral modes with $\omega_i=0$. As evident from Eq. (10), there can be no modes with $\omega>\omega_{p2}$ or $\omega<\omega_{p1}$ since this would make the RHS of the equation positive. Hence, if the neutral do exist, their frequency satisfies $\omega_{p1}<\omega<\omega_{p2}$. Since the plasma frequency is monotonic between $x=0$ and $x=x_{\max}$, there exists a location x_r, where $\omega=\omega_p(x_r)$, and the singular integral in the Eq. (10) can be expressed as

$$\text{RHS}=-(\omega_{p2}^2-\omega^2)\int_0^{x_{\max}}dx\left(\frac{\omega_p^2(x)}{c^2}|\psi|^2+\left|\frac{d\psi}{dx}\right|^2\right)\times\left(P\frac{1}{\omega^2-\omega_p^2(x)}\mp i\pi\delta(x-x_r)\frac{1}{|\omega_p^{2\prime}(x_r)|}\right), \tag{11}$$

where $\pm$ corresponds to ω approaching the real axis from above or from below, respectively. Since the imaginary part of the LHS of Eq. (10) vanishes, so should the imaginary part of Eq. (11), implying that either (i) both ψ and its derivative vanish at $x=x_r$ (trivial solution), or (ii) $|\omega_p^{2\prime}(x_r)|=\infty$ (infinitely sharp interface).

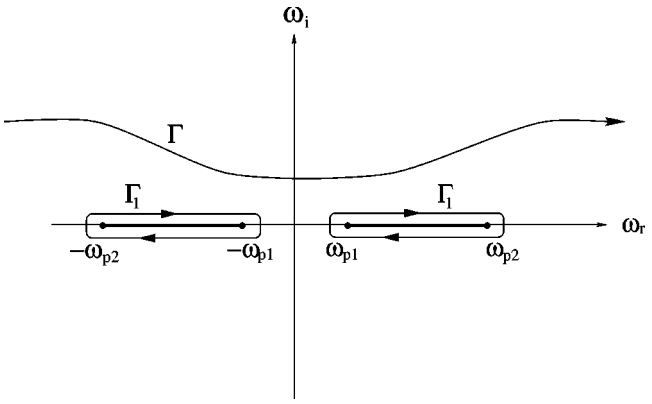

FIG. 1. Γ is the integration path for Eq. (12). Integral along the contour Γ can be reduced to a sum of two integrals along branch cuts (contours Γ_1).

While the trivial solution is of no interest, infinitely sharp interface is encountered, for example, in an ideal hollow channel. This is in agreement with the calculation of Sec. II which demonstrated that an ideal hollow channel supports a neutral edge mode. However, if electron density is continuous, there are no continuous neutral normal modes. Therefore, the surface mode disappears as soon as the step-function density profile of an ideal hollow channel is smoothed out. This conclusion disagrees with our earlier analytical and numerical findings, presented in Refs. 22, 23, which recovered weakly damped surface modes for thin channel walls. Section IV resolves this disagreement by calculating the Green's function of Eq. (6) and recovering the damped quasi-modes of a smooth plasma channel. As it turns out, these quasi-modes are discontinuous, so that there is no contradiction with Eq. (10).

IV. SOLUTION OF THE DRIVEN EQUATION

A. Construction of the Green's function

The magnetic field in the ζ-domain is then obtained by inverse Laplace transforming $\tilde{B}_y(x,\omega)$ along any contour Γ in the upper half plane of complex ω, as shown in Fig. 1:

$$B_y(x,\zeta)=\int_\Gamma \frac{d\omega}{2\pi} e^{-i\omega\zeta}\,\tilde{B}_y(x,\omega). \tag{12}$$

Magnetic field $\tilde{B}_y$ is computed by constructing the Green's function $G(x,x',\omega)$ of the operator $\mathcal{L}_S$, satisfying the boundary conditions at $x=0$ and $x=x_{\max}$, and a differential equation $\mathcal{L}_S\, G(x,x',\omega)=\delta(x-x')$. Such an approach was originally used by Briggs *et al.* to study the eigenmodes of a strongly magnetized non-neutral plasma.[28] By causality, we require that $G(x,x',\omega)$ has no singularities in the upper half ω-plane. The Green's function of $\mathcal{L}_S$ is

$$G(x,x',\omega)=\begin{cases} \dfrac{1}{D(\omega)}\phi_+(x,\omega)\phi_-(x',\omega) & \text{for } x'<x \\ \dfrac{1}{D(\omega)}\phi_-(x,\omega)\phi_+(x',\omega) & \text{for } x'>x, \end{cases} \tag{13}$$

where ϕ_- and ϕ_+ are linearly independent solutions of

$$\mathcal{L}_S\phi_\pm=0, \tag{14}$$

satisfying their respective boundary conditions: $\phi_-(x=0,\omega)=0$ and $\phi'_+(x=x_{\max},\omega)/\phi_+(x=x_{\max},\omega)=-\omega_{p2}/c$. Constant $D(\omega)$ is the Wronskian of $\phi_\pm$, given by $D(\omega)=[\phi'_+\phi_- - \phi'_-\phi_+]/\epsilon$. $D(\omega)$ will be referred to as the dispersion function because its zeros correspond to the channel eigenmodes. For example, for an ideal hollow channel $D(\omega_{\rm ch})=0$.

For any real x magnetic field can be calculated according to

$$\tilde{B}_y(x,\omega)=\int_0^{x_{\max}} dx' G(x,x',\omega)\left(\frac{\omega^2}{c^2}\frac{\epsilon'}{\epsilon^2}\tilde{f}(x',\omega)\right). \tag{15}$$

Similar Green's functions can be derived for the accelerating and transverse components of the electric field $\tilde{\mathcal{E}}_z$ and $\tilde{\mathcal{E}}_x$:

$$G_z(x,x',\omega)=i\frac{c}{\omega\epsilon(x,\omega)}\frac{\partial G(x,x',\omega)}{\partial x}, \tag{16}$$

$$G_x(x,x',\omega)=\frac{1}{\epsilon(x,\omega)}G(x,x',\omega). \tag{17}$$

The linearly independent solutions ϕ_- and ϕ_+ can be expressed in terms of the regular and singular solutions ϕ_r and ϕ_s in the vicinity of the complex singular point x_r. The regular solution can be expanded in the vicinity of x_r:

$$\phi_r(x)=(x-x_r)^2[1+k_p^2(x-x_r)^2/8+\cdots], \tag{18}$$

and the singular solution can be constructed in terms of the regular solution:

$$\phi_s(x)=\phi_r(x)\int_0^x \frac{dx'}{\phi_r^2(x')}\epsilon(x'). \tag{19}$$

The singular solution has a branch point at $x=x_r$. Since any pair of linearly independent basis functions can be constructed as a linear combination of ϕ_r and ϕ_s, at least one of the basis functions has a branch point at x_r.

Choosing ϕ_r and ϕ_s as the basis functions is convenient for analysis but not at all necessary for practical computations. For $\omega_i>0$ the eigenfunctions ϕ_- and ϕ_+ can be expressed in terms of any pair of linearly independent solutions of the homogeneous equation $\mathcal{L}_S\phi=0$. One such example is a set (ϕ_0,ϕ_1), satisfying $\phi_0(0)=0$, $\phi'_0(0)=1$, and $\phi_1(0)=\epsilon(x=0,\omega)$, $\phi'_1(0)=0$. Integrating these solutions according to Eq. (14) between $x=0$ to $x=x_{\max}$ yields both the dispersion function

$$D=\frac{\phi'_0(x_{\max})+k_{p2}\phi_0(x_{\max})}{\phi'_1(x_{\max})+k_{p2}\phi_1(x_{\max})}, \tag{20}$$

and the $\phi_\pm$ basis functions: $\phi_-=\phi_0$ and $\phi_+=\phi_0-D(\omega)\phi_1$. Integration of the homogeneous equation along the real axis is unambiguous for $\omega_i>0$ since the singularities of $\mathcal{L}_S$ lie above the real x-axis. From the results of the previous section, $D(\omega)=0$ has no roots if $\omega_p(x)$ is a monotonic continuous function. Alternatively, one might obtain ϕ_- directly by integrating Eq. (14) *forward* in x, starting from x

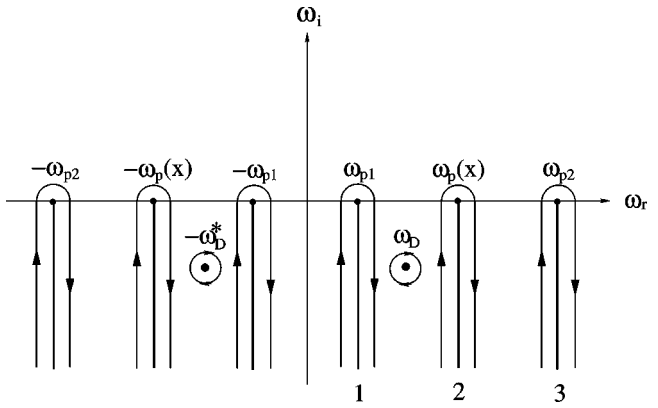

FIG. 2. A different cut which recovers the quasi-modes ω_D and ω_D^*-zeros of the analytic continuation of the dispersion function $D_*(\omega)$.

$=0$ (where the boundary conditions for ϕ_- are set). Similarly, ϕ_+ is obtained by integrating Eq. (14) *backwards* in x, starting from $x=x_{\max}$.

B. Analytic continuation of the Green's function

Singularities of $\mathcal{L}_S$ are encountered when ω assumes a real value from the interval $[\omega_{p1},\omega_{p2}]$. The dispersion function $D(\omega)$ thus has branch points at ω_{p1} and ω_{p2}. In addition, there is another branch point of the singular function $\phi_s(x,\omega)$ at $\omega=\omega_p(x)$. Hence, one can ensure that $B_y(x,\omega)$ is single-valued by making a single cut between ω_{p1} and ω_{p2}. The integration contour Γ can then be wrapped around the cut, as shown in Fig. 1. A similar cut must be made between $-\omega_{p2}$ and $-\omega_{p1}$.

However, integration around the branch cut in Fig. 1 does not reveal any information about the damped quasi-modes. A different cut, shown in Fig. 2, can be used to recover the quasi-modes. Following Ref. 28, the integration contour is pushed into the lower half plane. To do that, $D(\omega)$, $\phi_-(x,\omega)$, and $\phi_+(x,\omega)$ have to be analytically continued for $\omega_i<0$. Although $D(\omega)$ has no zeros above or below the real ω axis, its analytic continuation $D_*(\omega)$ may have zeros ω_D and $-\omega_D^*$ in the lower half-plane, as shown in Fig. 2. This phenomenon is analogous to the collisionless Landau damping of electrostatic plasma waves. The dielectric constant of the warm plasma does not vanish for any complex frequency, but its analytic continuation does, resulting in Landau-damped quasi-modes.

Not only the dispersion function $D(\omega)$, but also the basis functions $\phi_\pm(x,\omega)$ need to be analytically continued. Analytic continuation involves integrating the basis functions [i.e., solving the homogeneous differential equation (14)] along a contour which is no longer a straight line along the real axis. To illustrate the considerations that go into choosing the appropriate integration path, assume that ω belongs to the original contour Γ, i.e., $\omega=\omega_r+i\omega_i$, where $\omega_i>0$. The complex resonant point x_r is then located in the upper half of the x-plane.[35] For example, $\phi_-(x,\omega)$ is computed by integrating Eq. (14) along any contour, which connects the origin and x (including the straight line, of course), provided that the contour always stays below the resonant

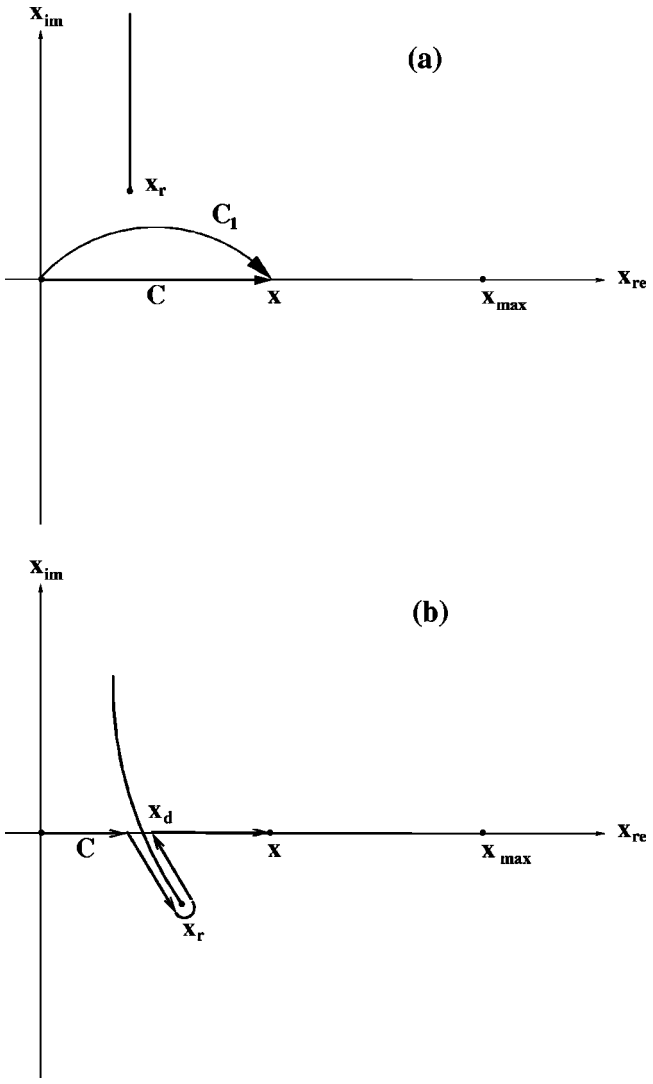

FIG. 3. Integration paths in the complex x plane of the differential equation $\mathcal{L}_S(\omega)\phi_{0,1}=0$ for the basis functions ϕ_0 and ϕ_1, whose boundary conditions are set at $x=0$. x_r is the resonance point, defined by $\epsilon(x_r,\omega)=0$. (a) ω in the upper half plane, Im $\omega>0$. C_1 and C-possible integration paths. Basis functions are continuous on the real axis. (b) ω in the lower half plane, Im $\omega<0$. Integration contour remains below the resonance point x_r to ensure analytic continuation of the Green's function. Basis functions are discontinuous on the real axis at $x=x_d$, where $\epsilon(x_d,\text{Re }\omega)=0$.

point $x_r(\omega)$. The analyticity of $\phi_-(x,\omega)$ in the complex x-plane is ensured by making a branch cut, as shown in Fig. 3(a).

When ω is moved into the lower half-plane, the resonant point $x=x_r(\omega)$ is also lowered below the real axis, making the integration of the homogeneous equation (14) along the real axis impossible as soon as x_r crosses the real axis. To ensure the analyticity of $\phi_\pm(x,\omega)$ as a function of ω, the integration contour in the complex x-plane must be deformed to stay *below* the branch point $x=x_r(\omega)$. Such a contour avoids the branch cut in the complex x-plane, as shown in Fig. 3(b).

To illustrate the choice of the appropriate branch cut in the x-plane, we first calculate $x_d(\omega)$, the intersection of the branch cut with the real axis. Basis functions undergo a jump when x moves from $x_d(\omega)-\varepsilon$ to $x_d(\omega)+\varepsilon$. To calculate

$x_d(\omega)$, note that the cuts in the ω plane are vertical for any fixed x. Basis functions undergo a discontinuous change when ω crosses the vertical cut which runs downward from $\omega_p(x_d)$. Therefore, the discontinuity point $x_d(\omega)$ is found by solving $\omega_p(x_d)=\mathrm{Re}\,\omega$. Note that $x_d(\omega)$ does not correspond to any physical discontinuity. As was earlier pointed out in the literature,[28,27] the discontinuity of the field is not ''real'' in the sense that it only exists in the frequency domain. The field discontinuity disappears after the integration over ω. Moreover, $x_d(\omega)$ depends on the choice of the branch cuts in the ω plane. The prescription for calculating x_d, given above, is consistent with vertical cuts in the complex frequency plane.

This analysis can now be generalized to construct the entire branch cut in the complex x plane, connecting the $x_d(\omega)$ and $x_r(\omega)$ endpoints. The cut consists of a set of points x_c, such that $\omega_p(x_c)=\mathrm{Re}\,\omega+i\gamma_c$, where $\mathrm{Im}\,\omega<\gamma_c<0$. It is, essentially, the mapping of the branch cut 2 of the complex ω plane onto the complex x plane according to $\omega_p(x_c)=\omega_c$, where ω_c belongs to the branch cut 2. Therefore, the shape of the cut in the complex x plane is entirely determined by the choice of the cut in the complex ω-plane. In other words, choosing a different cut 2 in Fig. 2 would result in a different cut in the x plane for the same value of ω.

Basis functions $\phi_{\pm}(x,\omega)$ undergo a discontinuity on the real axis at $x=x_d(\omega)$ for *any* ω in the lower half plane with $\omega_{p1}<\mathrm{Re}\,\omega<\omega_{p2}$. The particularly important frequencies are the poles of the analytically continued Green's function at $\omega=\omega_D$. They correspond to the zeros of the analytically continued dispersion function: $D_*(\omega_D)=0$. It can be shown that zeros of D_* come in pairs $(\omega_D,-\omega_D^*)$, as illustrated in Fig. 2. As explained in Sec. V, these poles define the collisionlessly damped quasi-modes of the plasma channel. Quasi-modes are the generalizations of the true eigenmodes of the channels with discontinuous density profiles, such as the hollow channels. Real frequencies and damping rates of these quasi-modes are independent of the choice of branch cuts in the ω plane. The existence of the quasi-modes does not contradict the findings of Sec. III, where it was demonstrated that $D(\omega)$ does not have zeros for any ω. The analytical proof of Sec. III relied on the continuity and differentiability of the hypothetic eigenfunction ψ of the homogeneous equation (14). Since the analytically continued basis functions $\phi_{\pm}(x,\omega_D)$ are discontinuous at $x_d(\omega_D)$, this proof is no longer valid.

With the procedures for the analytic continuation of the basis functions and the dispersion function $D(\omega)$ established, the inverse Laplace transform integration, given by Eq. (12), can be carried out along the branch cuts and around the poles of the analytically continued Green's function, as shown in Fig. 2. Contributions of the quasi-modes are important for the short-time evolution of the plasma wakes, $\zeta<1/\mathrm{Im}(\omega_D)$. For longer times quasi-modes damp out, and branch cut contributions dominate. This is because the fields, associated with the branch cuts, *algebraically* decay in ζ. Moreover, for very wide plasma channels quasi-modes are important in a very small part of the channel, and the branch cut 2 dominates throughout the rest of the channel. In the rest of the paper we separately consider the global quasi-modes and the local plasma excitations, associated with the branch cut 2.

V. WEAKLY DAMPED QUASI-MODES

The origin of the weakly damped quasi-modes in inhomogeneous plasma can be best understood by considering a plasma channel with an infinitely sharp interface between the two regions of different plasma density. An example of such a channel—hollow plasma channel—was recently considered as a possible candidate for a plasma-based particle accelerator due to the attractive properties of the accelerating and focusing fields inside the evacuated channel.[20–23] Hollow plasma channel supports a surface mode which peaks at the vacuum-plasma interface and exists both inside the channel and in the plasma (within a collisionless skin-depth from the vacuum-plasma interface). This electromagnetic surface mode is a true eigenmode of the plasma channel, with a vanishing damping coefficient and frequency $\omega_{\mathrm{ch}}=\omega_{p0}/\sqrt{1+k_{p0}b}$. The surface mode is decoupled from the bulk plasma modes because its frequency is different from the bulk plasma frequency ω_{p0}. Simply put, there are no electrostatic plasma modes with frequency ω_{ch} that could strongly couple to the surface mode.

As the plasma-vacuum interface is smoothed out, the surface mode couples to the continuum of the electrostatic plasma waves. Now there exists a resonant location x_r, such that $\omega_p(x_r)=\omega_{\mathrm{ch}}$, and coupling between the electrostatic plasma wave, localized at x_r, and the surface mode leads to the damping and frequency shift of the latter. Similarly to the surface modes of infinitely sharp plasma channels, quasi-modes are peaked in the neighborhood of x_r and decay exponentially away from x_r. Quasi-modes are distinct from the localized electrostatic plasma waves in that they are global (i.e., exist throughout the plasma), yet possess a well-defined frequency which is independent of the transverse location x. The difference between the weakly damped quasi-modes and the ''true'' surface modes is that the latter ones are the real undamped eigenmodes, whereas the former ones belong to the continuum of the plasma waves. Weakly damped quasi-modes are important only for short times of order the damping time, after which the coherent, single-frequency motion of the plasma electrons is destroyed, and the local fields, oscillating with the local plasma frequencies $\omega_p(x)$, prevail.

Frequencies of the quasi-modes are defined by the zeros of the analytic continuation of the dispersion function: $D_*(\omega_D)=0$. The numerical procedure for calculating $D_*(\omega)$ consists of several steps. First, for a given ω in the lower half-plane, the resonant point $x_r(\omega)$ is calculated. A contour, which passes below x_r and connects the endpoints $x=0$ and $x=x_{\max}$ [as shown in Fig. 3(b)] is then chosen in the complex x-plane. Next, two linearly independent solutions (e.g., ϕ_0 and ϕ_1) are integrated along this contour from $x=0$ to $x=x_{\max}$. The dispersion function is then given by Eq. (20). Complex frequency ω can now be scanned to find zeros of D_*.

The contribution of the quasi-mode to the magnetic field at the transverse location x is given by

$$B^{(p)}(x,\zeta)=\frac{i}{D'_*(\omega_D)}e^{-i\omega_D\zeta}\phi_-(x,\omega_D)\int_0^\infty dx'\,\phi_-(x',\omega_D)\times\left(-\frac{\omega_D^2}{c^2}\frac{\epsilon'(x',\omega_D)}{\epsilon^2(x',\omega_D)}\tilde{f}(x',\omega_D)\right). \quad (21)$$

Equation (21) loses validity in the immediate vicinity of $x=x_d(\omega_D)$. The contribution of the branch cut 2, shown in Fig. 2, generates fields at the frequency of the quasi-mode, and needs to be taken into account. This could be anticipated since the pole contribution to the magnetic field $B^{(p)}(x,\zeta)$ is discontinuous at $x=x_d(\omega_D)$, whereas the total magnetic field must be continuous.

As an example, consider parabolic plasma channels

$$\omega_p^2(x)=\omega_{p1}^2+\frac{(\omega_{p0}^2-\omega_{p1}^2)x^2}{x^2+b^2}, \quad (22)$$

of two types: (a) hollow on axis ($\omega_{p1}=0$), or (b) with finite on-axis density ($\omega_{p1}\neq 0$). Such locally parabolic density profiles have been experimentally generated[10] to guide laser pulses through the plasma. For such channels $D_*(\omega)$ is found from Eq. (20), where the basis functions $\phi_{0,1}$ are numerically integrated from $x=0$ to $x=x_{\max}$ along the contour shown in Fig. 2(b). Parabolic channels are the easiest from the standpoint of the numerical integration: only one complex resonant point $x_r(\omega)$ exists in the lower half of the complex x-plane. This simplifies the choice of the integration contour, which was taken as a sum of two straight lines in the complex plane: one, connecting $x=0$ and $x=x_r(\omega)-i\nu$ (where ν is an arbitrary positive number) and the other, connecting $x=x_r(\omega)-i\nu$ and $x_{\max}$ (chosen at $x_{\max}=3b$). The real frequency and the damping rate of the quasi-modes of are plotted as functions of the dimensionless channel width $k_{p0}b$ in Figs. 3(a) and 3(b). We observe that for both types of plasma channels, with and without plasma on axis, there exists a single quasi-mode which becomes localized near the origin as the channel widens. Note that even for the wide ($k_{p0}b>1$) plasma channels the damping rate of the quasi-mode is much smaller than the real frequency.

For a hollow channel the only contribution to the accelerating gradient $E_z(x=0)$ comes from the quasi-mode. A fluid code, which calculates all the electromagnetic fields and plasma fluid quantities as a function of ζ, was recently developed.[36] To extract the damping coefficient and the frequency from the fluid code, we fitted $E_z(x=0,\zeta)$ by $E_0\cos(\omega_r\zeta+\phi_0)\exp(-\gamma\zeta)$, where E_0 and ϕ_0 are constants. We then compared ω_r and γ, the fit parameters of the fluid simulation, with the complex frequency ω_D from Fig. 3(a). For a wide range of the channel widths $k_{p0}b$ we found an exact agreement between the two approaches: the analytic continuation of the Green's function in the frequency domain and the numerical simulation in time domain.[36]

In Sec. VII we demonstrate that $D_*(\omega)$ does not vanish, provided that the plasma is almost homogeneous $k_pL\gg 1$, where $L=\omega_p(x)/\omega_p'(x)$ is the inhomogeneity scale of the plasma density, evaluated at the ''resonant'' x such that $\epsilon(\omega,x)=0$. As Fig. 4(a) indicates, the quasi-modes of the plasma channel, described by Eq. (22), persist even for $k_{p0}b\gg 1$. If the inhomogeneity length L of the channel is

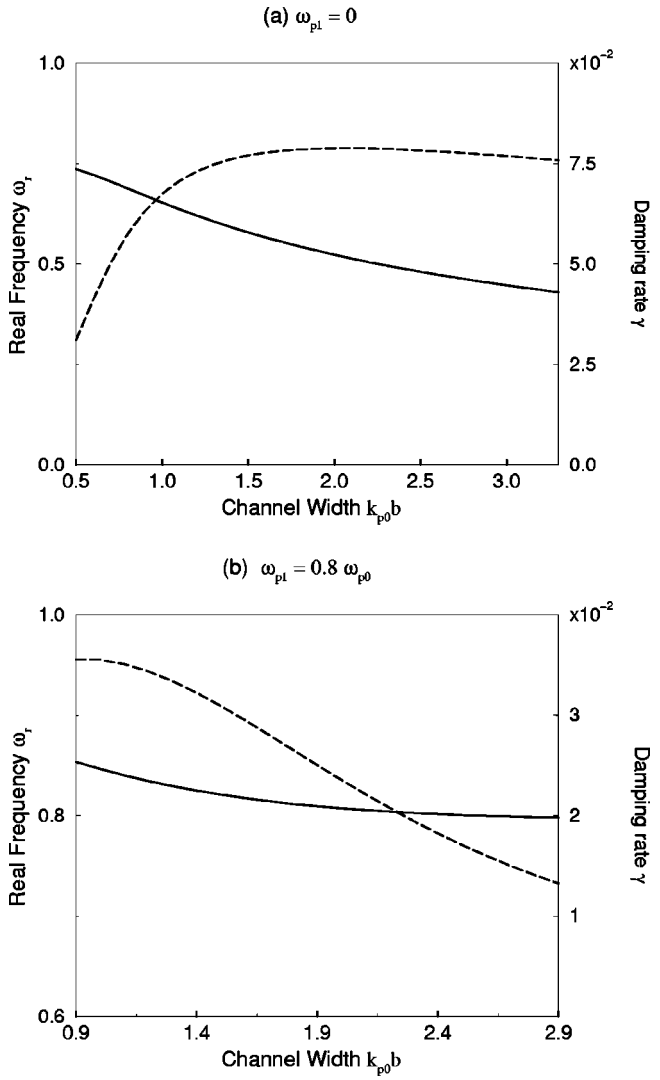

FIG. 4. The quasi-mode's real frequency Re(ω_D) (solid line) and damping rate Im(ω_D) (dashed line) as a function of the channel width $k_{p0}b$ for two types of plasma channels: (a) zero plasma density on axis and (b) finite plasma density on axis. Plasma frequency satisfies $\omega_p^2(x)=\omega_{p1}^2+(\omega_{p0}^2-\omega_{p1}^2)x^2/(x^2+b^2)$.

proportional to b (which would be the case if the resonant point always remained somewhere around $x=b$), the existence of the quasi-modes would contradict the earlier statement about $D_*(\omega)$ in almost homogeneous plasma. This contradiction is resolved by noticing that the real frequency of the quasi-mode decreases with increasing $k_{p0}b$. Thus, the resonant location x_r shifts towards the origin with increasing channel size. In fact, for $x_r\ll b$ the channel density can be assumed as given by

$$\omega_p^2(x)=\omega_{p0}^2x^2/b^2. \quad (23)$$

The frequency of a quasi-mode of such a channel must be expressed as a function of ω_{p0}/b and the speed of light c. The only dimensionally correct combination is

$$\omega_D=P\left(\frac{\omega_{p0}c}{b}\right)^{1/2}, \quad (24)$$

where P is a complex constant which has to be determined numerically by solving the eigenvalue equation

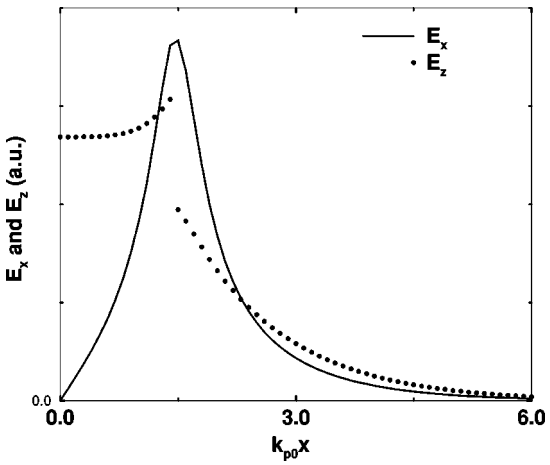

FIG. 5. Spatial profiles of the focusing (solid line) and accelerating (black circles) electric fields of the collisionlessly damped quasi-mode of a wide plasma channel. Plasma frequency satisfies $\omega_p^2(x)=\omega_{p0}^2x^2/(x^2+b^2)$; channel width $k_{p0}b=3$. Accelerating field E_z of the quasi-mode is discontinuous at $x_d\approx 1.5k_{p0}^{-1}$.

$$\frac{d}{du}\left(\frac{1}{P^2-u^2}\frac{d\psi}{du}\right)=\frac{u^2}{P^2-u^2}\psi. \tag{25}$$

In Eq. (25) u is the normalized transverse displacement $u=\sqrt{\omega_{p0}/cb}x$, and the usual boundary conditions $\psi(0)=\psi(+\infty)=0$ are imposed. Equation (25) is integrated between $u=0$ and $u=+\infty$ along a contour in the complex u plane which passes below the singularity $u=P$. This numerical procedure yields a single value of $P=0.85-0.20i$. Thus, the quasi-mode of a parabolic channel is heavily damped, decaying by a factor e in less than one full oscillation.

VI. ASYMPTOTIC ANALYSIS OF WAKE EXCITATION

Contributions of the quasi-modes are not sufficient to describe the electromagnetic wakes for all times and at all transverse locations inside the plasma channel. The quasi-mode contribution to the total electromagnetic fields at a given transverse point can be negligible if the quasi-mode is localized far away from that location. For example, the field components of the wide channel quasi-mode become exponentially small sufficiently far away from the resonance point. Consider the spatial profiles of the accelerating and focusing electric fields, shown in Fig. 5, which correspond to the quasi-mode of the parabolic hollow channel $\omega_p^2(x)=\omega_{p0}^2x^2/(x^2+b^2)$ with $k_{p0}b=3$. Both fields peak at $x_d(\omega_D)\approx 1.5/k_{p0}$, where $\omega_D=\omega_{p0}(0.45-0.077i)$ is the complex frequency of the quasi-mode. The values of both fields at the edge of the channel ($x=2b$) are negligible in comparison with their peak values at $x=x_d$. Note that the accelerating field, corresponding to the quasi-mode, is discontinuous at x_d. As explained in Sec. V, this does not correspond to a physical discontinuity. In addition to being localized, quasi-modes exponentially decay with ζ, practically disappearing several decay times $1/\mathrm{Im}\,\omega_D$ after the passage of the laser pulse.

Under these circumstances the contributions from the branch cuts 1–3, shown in Fig. 2, can become very important. The contributions of the cuts 1 and 3 are very distinct from those of the cut 2. Mathematically, cuts 1 and 3 are the branch cuts of the dispersion function $D_*(\omega)$. Basis functions $\phi_\pm(x,\omega)$ are continuous across these cuts for all $0<x<x_{\max}$. Physically, cuts 1 and 3 describe the electromagnetic fields generated at the edges of the plasma ($x=0$ and $x=x_{\max}$), which penetrate by about a collisionless skin depth into the bulk of the plasma. These fields resemble the quasi-mode in that they too are highly localized. However, for $\zeta>\tau_m$, where τ_m is the phase-mixing time

$$\tau_m=\frac{\omega_p}{c\omega_p'}, \tag{26}$$

these contributions decay algebraically with time. For shorter times $\zeta\ll\tau_m$ these fields are proportional to the powers of ζ/τ_m. Therefore, cuts 1 and 3 do not contribute if the plasma channel has vanishing density gradients at the edges, as it is the case for the parabolic channels, described by Eq. (22). Since for the majority of smooth and symmetric plasma channels cuts 1 and 3 are not important, they are not considered in this paper.

Basis functions $\phi_\pm(x,\omega)$ are discontinuous across the cut 2, the contribution from which describes the locally excited electromagnetic fields, oscillating with the the local plasma frequency $\omega_p(x)$. The contribution from the cut 2 is significant whenever the ponderomotive excitation extends to x, or there is a nonvanishing initial perturbation at x. Since the Green's function of the magnetic field $G(x,x',\omega)$ does not have a pole at $\omega=\omega_p(x)$, cut 2 provides the only contribution to the locally excited magnetic field. The locally excited electric fields E_z and E_x have three sources: the local electric field, described by the first term in the RHS of Eq. (3), pole contributions at $\omega=\omega_p(x)$, and the cut 2 contribution.

Let us calculate the inverse Laplace transform of $\tilde{B}_y(x,\omega)$ along the branch cut 2 in the vicinity of $\omega=\omega_p(x)$. For simplicity, assume that x is removed from the ''discontinuity'' point $x_d(\omega_D)$. This is equivalent to assuming that the cut 2 does not cross the quasi-mode frequency ω_D. Integrals along the two sides of the cut 2 do not cancel because the Green's function is discontinuous across the branch cut (although the dispersion function $D_*(\omega)$ remains continuous). It is convenient to separate the integration path in the complex x' plane into three separate intervals: $\mathcal{C}_-$ between 0 and $x_r-i\varepsilon$; $\mathcal{C}$ between $x_r-i\varepsilon$ and x; $\mathcal{C}_+$ between $x_r-i\varepsilon$ and $x_{\max}$. The Laplace transformed magnetic field is thus separated into two contour integrals: $\mathcal{I}_1$ along the contours $\mathcal{C}_-$ and $\mathcal{C}_+$, and $\mathcal{I}_2$ along the contour $\mathcal{C}$. Assuming that the ponderomotive potential is nearly homogeneous in the vicinity of x, f can be brought outside of the integral.

The separate contributions are then given by

$$I_1=\frac{\omega_p^2\tilde{f}(x,\omega_p)}{c^2D_*(\omega_p)}\left[\phi_+(x)\int_{\mathcal{C}_-}dx'\,\phi_-(x')\frac{\epsilon'}{\epsilon^2}+\phi_-(x)\int_{\mathcal{C}_+}dx'\,\phi_+(x')\frac{\epsilon'}{\epsilon^2}\right] \tag{27}$$

and

$$I_2=\frac{\omega_p^2\tilde{f}(x,\omega_p)}{c^2D_*(\omega_p)}\left[\phi_+(x)\int_{\mathcal{C}}dx'\,\phi_-(x')\frac{\epsilon'}{\epsilon^2}-\phi_-(x)\int_{\mathcal{C}}dx'\,\phi_+(x')\frac{\epsilon'}{\epsilon^2}\right], \tag{28}$$

where $\omega_p\equiv\omega_p(x)$. We are interested in the changes in I_1 and I_2 as the frequency moves across the cut 2. In I_1 this change comes about from the jump in $\phi_\pm(x)$, yielding

$$\delta I_1=\frac{\omega_p^2\tilde{f}(x,\omega_p)}{c^2D_*(\omega_p)}\delta\phi_s(x)\int_{\mathcal{C}_-+\mathcal{C}_+}dx'\,\phi_{(\pm)}\frac{\epsilon'}{\epsilon^2}, \tag{29}$$

where $\phi_{(\pm)}=\phi_-$ on $\mathcal{C}_-$ and $\phi_{(\pm)}=\phi_+$ on $\mathcal{C}_+$. It can be shown, using Eqs. (18), (19), that the jump of the singular solution ϕ_s across the $x-x_r$ cut is given by

$$\delta\phi_s(x)=\frac{\pi i\epsilon' k_p^2}{2}\phi_r(x), \tag{30}$$

where both ϵ' and k_p are evaluated at $x=x_r$.

Two factors contribute to the change in I_2: first, the basis functions $\phi_\pm(x)$ change (just as in I_1), and, second, the values of the integrals along the contour $\mathcal{C}$ also change. This is because when ω is to the left (right) of the cut 2, the integration contour $\mathcal{C}$ lies to the left (right) of the $x-x_r$ cut. The singular solution ϕ_s is discontinuous across the $x-x_r$ cut, and so are the basis functions $\phi_\pm$. Using the expression for the jump of the singular solution ϕ_s across the $x-x_r$ cut, given by Eq. (30), it is a matter of straightforward (although lengthy) algebra to demonstrate that the two factors cancel, so that I_2 is continuous across the cut 2: $\delta I_2=0$.

Assuming that $\omega=\omega_p(x)-i\nu$, where $\nu\ll\omega_p$, the complex resonant point x_r is determined by

$$(x-x_r)=i\frac{2\nu}{\omega_p(x)\epsilon'(x,\omega_p)}. \tag{31}$$

The small-argument expansion of the ϕ_r, given by Eq. (18), is valid if $k_p(x-x_r)\ll 1$, which translates into $\nu\ll c\epsilon'$. Since only the frequencies with $\nu<1/\zeta$ effectively contribute to the integral along the cut 2, Eq. (18) is valid for $\zeta\gg\max[1/(c\epsilon'),1/\omega_p]$. Physically, this corresponds to the times longer than than the longest of the plasma period and the phase-mixing time τ_m.

Substituting Eq. (31) into Eq. (27), and integrating $\tilde{B}(x,\omega)$ over ν yields

$$B(x,\zeta)\approx e^{-i\omega_p(x)\zeta}\frac{2k_p^2c\epsilon'^2}{D_*(\omega_p)}\left(\frac{1}{c\epsilon'\zeta}\right)^3\times\int_{\mathcal{C}_-+\mathcal{C}_+}dx'\,\phi_{(\pm)}\frac{\epsilon'}{\epsilon^2}\tilde{f}(x',\omega_p). \tag{32}$$

In Eq. (32) the powers of ϵ' were combined to emphasize that the generated magnetic field is proportional to the plasma inhomogeneity ϵ'. This is because the bracketed term is required to be much smaller than unity in order for the Eq. (32) to be valid. The contour integral in Eq. (32) cannot be analytically evaluated for a general plasma profile. However, when plasma inhomogeneity is weak, $k_pL\gg 1$, the contour integral can be analytically calculated. Moreover, the restriction of the very large time can be removed, enabling the calculation of $B(x,\zeta)$ for arbitrary $\zeta\gg 1/\omega_p$. The results of this calculation are presented in Sec. VII.

Using Eqs. (16), (17), the long-time behavior of the accelerating electric fields can be similarly evaluated by splitting the integration path into three contours, $\mathcal{C}$, $\mathcal{C}_-$, and $\mathcal{C}_+$. The important difference in the calculations of the electric and magnetic fields is that $\tilde{E}_z(x,\omega)$ has a pole at $\omega=\omega_p(x)$. One can demonstrate that the contribution of the pole exactly cancels the z-component of the first term in the RHS of the Eq. (3). The remaining accelerating field decays according to

$$E_z(x,\zeta)\approx e^{-i\omega_p(x)\zeta}\frac{k_p^3c\epsilon'}{2D_*(\omega_p)}\left(\frac{1}{c\epsilon'\zeta}\right)\times\int_{\mathcal{C}_-+\mathcal{C}_+}dx'\,\phi_{(\pm)}\frac{\epsilon'}{\epsilon^2}\tilde{f}(x',\omega_p). \tag{33}$$

According to Eqs. (32), (33), the accelerating field decays slower than the magnetic field for $\zeta\gg\tau_m$.

Similarly, both the pole at $\omega=\omega_p(x)$ and the integral along the branch cut contribute to the focusing electric field E_x. Since the locally excited electric field, given by the x-component of first term in the RHS of the Eq. (3), is proportional to $\partial f/\partial x$, the ponderomotive potential in the integrand is expanded according to $f(x')\approx f(x)+f'(x)(x'-x)$. Unlike the case of the longitudinal field, the pole contribution does not cancel the local field, so that there is a nondecaying oscillating wakefield left in the plasma. Since magnetic field decays faster than the electric field, we see that, over time, the wake becomes predominantly electrostatic.

The time evolution of the electromagnetic wake in the plasma channel can be described as follows. Initially, a global quasi-mode is excited. Electromagnetic fields, associated with the quasi-mode, oscillate with a fixed frequency throughout the plasma. The oscillation amplitudes exponentially decay in time with the damping rate equal to the imaginary part of the quasi-mode frequency ω_D. For longer times local excitations prevail. At a given transverse position x these fields oscillate with the local plasma frequency $\omega_p(x)$. For the times longer than the phase-mixing time magnetic and electric fields algebraically decay in time according to different power laws, with magnetic field decaying the fastest, $B_y\propto\zeta^{-3}$, and the transverse electric field retaining a constant oscillation amplitude. More quantitative statements about the time dependence of the fields are made in Sec. VII for wide plasma channels, whose density varies slowly on the scale of the collisionless skin depth: $k_pL\gg 1$.

VII. WAKE EXCITATION IN WIDE PLASMA CHANNELS

A. Time evolution of local excitations

In Sec. VI the long-time ($\zeta\gg\tau_m$) asymptotic behavior of the electromagnetic wakes was evaluated. It turns out that the long-time restriction can be lifted, and the Green's func-

tion can be analytically integrated along the branch cut 2 (responsible for the local excitations) if simplifying assumptions are made about the plasma density and laser profiles. In this section we assume that the plasma is weakly inhomogeneous, so that the scale of the plasma inhomogeneity is much longer than the plasma wavelength: $k_p' \ll k_p^2$. The laser profile is also assumed only weakly nonuniform on a scale $1/k_p$: $\partial \ln|f|/\partial x \ll k_p$. The closed form expressions for the ϕ_+ and ϕ_- can be obtained, enabling the analytic calculation of the dispersion function $D_*(\omega)$ and the contour integral in Eq. (29).

In the vicinity of the resonant point, $|x-x_r| \ll L$ the lowest-order Taylor expansion for the plasma dielectric function can be used: $\epsilon = \epsilon'(x-x_r)$. Therefore, in the vicinity of x_r the basis functions $\phi_\pm$ satisfy

$$\frac{\partial^2 \phi}{\partial x^2} - \frac{1}{x-x_r}\frac{\partial \phi}{\partial x} - k_p^2 \phi = 0. \tag{34}$$

Equation (34) has two independent solutions:

$$\phi = tI_1(t) \quad \text{and} \quad \phi = tK_1(t), \tag{35}$$

where $k_p \equiv k_p(x)$, $t = k_p(x-x_r)$, and $I_1(t)$ and $K_1(t)$ are the modified Bessel functions.

Further assume that x is at least $1/k_p$ away from both the origin and the discontinuity point $x_d(\omega_D)$. The origin can now be treated as being infinitely far away, so that the integration in Eq. (28) can be carried out along the path which runs from $-\infty$ to $+\infty$, passing right under the resonant point x_r.

The next step is to construct the basis functions $\phi_\pm$, satisfying their boundary conditions at $\pm\infty$. For example, the second solution of the Eq. (34) $tK_1(t)$ vanishes as $t \to +\infty$. Of course, Eq. (34) is not valid for $|x-x_r| > L$, and neither are its solutions. However, since $k_p L \gg 1$ (wide channel), the true approximate solution becomes exponentially small for $L > |x-x_r| > 1/k_p$, so that the difference between the exact solution ϕ_+ and the approximate solution $tK_1(t)$ is exponentially small. The linear combination of the Bessel functions from Eq. (35), decaying as $x \to -\infty$, can also be constructed. Altogether, the basis functions are given by

$$\phi_- = tK_1(t) + i\pi tI_1(t) \quad \text{and} \quad \phi_+ = tK_1(t). \tag{36}$$

The dispersion function is then given by

$$D_* = \frac{k_p^2}{\epsilon'}\left(\frac{\phi_- d\phi_+/dt - \phi_+ d\phi_-/dt}{t}\right) = -\frac{i\pi k_p^2}{\epsilon'}. \tag{37}$$

Magnetic field $B_y(x,\zeta)$ is found by substituting $\phi_\pm$, D_*, and $\delta\phi_s = \delta\phi_+$ from Eqs. (36), (37) into Eq. (29) and integrating the result over ν. The jump of the basis functions across the cut is given by[37]

$$\delta\phi_+ = t[K_1(te^{i2\pi}) - K_1(t)] = 2i\pi tI_1(t). \tag{38}$$

By noting that $\phi_-(t) = \phi_+(-t)$, Eq. (29) can be integrated by parts and simplified to

$$\delta I_1 = -4t\epsilon' \int_{x_r}^{x_r+\infty} dx' \frac{\phi_+'}{\epsilon}, \tag{39}$$

where the plasma quantities, such as ϵ', are evaluated at $x = x_r$.

Since the basis function ϕ_+ is localized by $|x-x_r| < 1/k_p$, the dielectric function can be expanded in the vicinity of x_r as $\epsilon(x') = \epsilon'(x'-x_r)$. Substituting the expression for $\phi_+'/(x-x_r)$ from Eq. (34) into Eq. (39), obtain, after integrating by parts,

$$B_y(x,\omega) = 4tI_1(t)\omega/c \int_0^\infty dt \;\; tK_1(t) = 2\pi tI_1(t)\omega/c. \tag{40}$$

For the times longer than the local plasma period, $\zeta \gg 1/\omega_p(x)$, only the frequencies with $\nu \ll \omega_p(x)$ significantly contribute to the inverse Laplace transform integration, so that $t = k(x-x_r) \approx i(\omega_p/c)(\nu/\omega_p')$. Note, however, that although ω is always close to ω_p for weakly inhomogeneous plasmas, $|t|$ can be either small (for $\nu \ll c/L$), or large ($\nu \gg c/L$). These two limits correspond to the times longer or shorter than the phase-mixing time τ_m.

Integrating $B_y(x,\omega)$ along the contour 2 yields

$$\begin{aligned} B_y(x,\zeta) &= e^{-i\omega_p(x)\zeta}\int_0^\infty d\nu e^{-\nu\zeta} k f(x,\omega) tJ_1(it) \\ &\simeq -ie^{-i\omega_p(x)\zeta}\frac{\omega_p^2}{c^2\omega_p'}\tilde{f}(x,\omega_p) \\ &\quad \times \int_0^\infty d\nu e^{-\nu\zeta}\nu J_1\left(\frac{\omega_p}{c}\frac{\nu}{\omega'}\right). \end{aligned} \tag{41}$$

The integral in Eq. (41) can be evaluated exactly,[38] resulting in

$$B_y(x,\zeta) = -i\frac{k_p}{\tau_m}e^{-i\omega_p\zeta}\tilde{f}(x,\omega_p)\left[1+\frac{\zeta^2}{\tau_m^2}\right]^{-(3/2)}. \tag{42}$$

Combining this contribution of the cut $\omega = \omega_p(x) - i\nu$, $\nu > 0$ with the contribution from the symmetric cut $\omega = -\omega_p(x) - i\nu$, $\nu > 0$, yields the final expression for $B_y(x,\zeta)$ excited by a short laser pulse with a large spot size in a wide plasma channel:

$$B_y(x,\zeta) = -2\sin(\omega_p\zeta)\frac{k_p}{\tau_m}\tilde{f}(x,\omega_p)\left[1+\frac{\zeta^2}{\tau_m^2}\right]^{-(3/2)}. \tag{43}$$

The inverse Laplace transform of E_x and E_z can be done in a similar way. The main difference is that in the case of E_z there is a nonvanishing contribution to the x' integral from a pole at $x' = x$, which exactly cancels the locally driven field. After some algebra we find

$$\begin{aligned} E_x(x,\zeta) &= -\sin(\omega_p\zeta)\omega_p\frac{\partial\tilde{f}(x,\omega_p)}{\partial x}\left[1+\frac{\zeta^2}{\tau_m^2}\right]^{-3/2} \\ &\quad -\cos(\omega_p\zeta)\frac{\omega_p^2}{c}\tilde{f}(x,\omega_p)\frac{\zeta/\tau_m}{\sqrt{1+\zeta^2/\tau_m^2}}, \end{aligned} \tag{44}$$

$$E_z(x,\zeta) = \cos(\omega_p\zeta)\frac{\omega_p^2}{c}\tilde{f}(x,\omega_p)\frac{1}{\sqrt{1+\zeta^2/\tau_m^2}}, \tag{45}$$

where $\omega_p \equiv \omega_p(x)$ is the *local* plasma frequency at the transverse position x. In deriving Eqs. (43), (44), (45) the second and higher derivatives of f are neglected. Although the first term in Eq. (44) is proportional to $\partial f/\partial x$ and decays as ζ^{-3} for large times, it was kept because it is larger than the second term for $\zeta \ll \tau_m$.

In a homogeneous plasma the second term in Eq. (44) identically vanishes. Interestingly, in a channel the locally excited transverse electric field, described by the first term, rapidly decays with time, while the electromagnetic contribution, described by the second term, reaches the steady oscillation amplitude. This amplitude is *independent* of the transverse gradient of the ponderomotive potential. Also note that the nondecaying component of the focusing electric field is *in phase* with the accelerating field. This is potentially important for plasma-based particle accelerators. In a standard laser wakefield accelerator, based on a transversely uniform plasma, the accelerating and focusing electric fields are 90 degrees out of phase. Therefore, the phase region, where an injected particle is both accelerated and focused, is only $\lambda_p/4$ long. In a channel this region can be $\lambda_p/2$ long, as seen from Eqs. (44), (45). A qualitatively similar observation was made by Andreev *et al.*,[25] who earlier studied wake excitation in wide plasma channels for very short times $\zeta \ll \tau_m$.

Equations (43), (44), (45) constitute an important result of this paper. For the first time, to our knowledge, the closed form expressions for the wake evolution in wide plasma channels, valid for the arbitrary times, have been derived, and the phase-mixing time τ_m introduced. The physical meaning of the phase-mixing time, as well as the basic physics of the collisionless field decay in plasma channels, is explained below.

B. Phase-mixing in plasma channels

Damping of the electromagnetic fields in plasma channels is reminiscent of the decay of two-dimensional plasma oscillation due to the trajectories crossing, as described by Dawson.[39] To appreciate the differences of these two damping mechanisms, consider the underlying basic physics. Local plasma oscillations (and the corresponding electric field) decay when different plasma fluid elements, oscillating with their local plasma frequencies, get out of phase. Consider two fluid elements, initially located at $x = x_0$ and $x = x_0 + \Delta x$ and oscillating with their local plasma frequencies $\omega_p(x_0)$ and $\omega_p(x_0 + \Delta x)$, respectively. These two elements get out of phase after

$$\tau = |\omega_p' \Delta x|^{-1}. \tag{46}$$

Below we qualitatively argue for the appropriate Δx, which has to be substituted into Eq. (46).

Electrostatic cold plasma oscillations, considered by Dawson, collapse when adjacent fluid elements collide with each other. This is because there is no Pointing flux associated with such oscillations, so that the energy can only be transported from one position to the next by the plasma electrons. This results in the trajectory crossing, which can be interpreted as dephasing between the electrons separated by the distance equal to their oscillation amplitude A. Therefore, the nonlinear wave breaking time $\tau_{\mathrm{WB}} = |A\omega_p'|^{-1}$ is calculated by substituting $\Delta x = A$ into Eq. (46). For very small oscillation amplitudes the trajectory-crossing time becomes very long. This type of the transverse wave breaking, which takes place several plasma periods behind the laser pulse, was recently described by Bulanov *et al.*[40]

On the other hand, wakes in plasma channels are not purely electrostatic. There is a nonvanishing Pointing flux, associated with these wakes, which enables communication between different transverse positions. Locally excited plasma oscillations do not remain localized (and electrostatic) because of the finite magnetic field generated in the channel according to Eq. (43). This magnetic field produces a finite Pointing flux which spatially re-distributes the electromagnetic energy. As a result, electromagnetic wakes in the inhomogeneous plasma become nonlocal: fields at a given spatial location x are affected by the plasma currents within a collisionless skin depth c/ω_p from x. Therefore, wakes damp when, roughly, two fluid elements, separated by c/ω_p, get out of phase. Substituting $\Delta x = c/\omega_p$ into Eq. (46) results in $\tau_m = \omega_p/c\omega_p'$. Below we demonstrate how this estimate can be obtained in a more formal way.

As Eqs. (43), (44), (45) indicate, magnetic field decays faster than both components of the electric field. This implies that, by conservation of the total vorticity,[32]

$$\nabla \times \mathbf{v} = \frac{e\mathbf{B}}{mc}, \tag{47}$$

so that for large times $\nabla \times \mathbf{v} \approx 0$, and the plasma flow becomes almost curl-free. This property of the flow helps understand why the axial electric field is much smaller than the transverse electric field for large times. The curl-free flow condition for $\zeta \gg \tau_m$ implies $\partial v_z/\partial x = \partial v_x/\partial z$, or $v_z = -v_x \tau_m/\zeta$. The same relationship exists between the axial and transverse components of the electric field, as can be observed from Eqs. (44), (45). Combining Maxwell's equations with Eq. (47) yields

$$\left[\frac{\partial^2}{\partial x^2} - k_p^2(x)\right] B_y \approx \frac{4\pi e n_0}{c^2 \zeta} \hat{v}_x e^{-i\omega_p(x)\zeta} + \text{c.c.}, \tag{48}$$

where we have used the curl-free flow assumption and the fact that, for large ζ, v_x oscillates with a constant amplitude $2\hat{v}_x$.

Assuming that the plasma density does not significantly change on a scale of the collisionless skin depth, Eq. (48) can be solved in closed form by expanding $\omega_p(x') \approx \omega_p(x) + \omega_p'(x' - x)$:

$$B_y(x,\zeta) = -\frac{2\pi e n_0 \hat{v}_x}{k_p c^2 \zeta} e^{-i\omega_p(x)\zeta} \times \int_{-\infty}^{+\infty} dx' e^{-k_p|x-x'|} e^{i\omega_p' \zeta (x-x')} + \text{c.c.} \tag{49}$$

As illustrated by the integrand of Eq. (49), fluid elements within one collisionless skin depth from x contribute to $B_y(x)$. For large ζ these contributions get out of phase, and the integral in Eq. (49) decays as $(1 + \zeta^2/\tau_m^2)^{-1}$. Therefore, magnetic field decays as ζ^{-3}, in agreement with Eq. (43).

This calculation illustrates how the electromagnetic nature of the channel wake results in the nonlocal excitation on a c/ω_p scale, leading to phase-mixing of the plasma fluid and algebraic decay of the wake.

If the plasma oscillation amplitude A is much smaller than the collisionless skin depth, phase mixing occurs before the wave breaking. Transverse wave breaking can still take place after $\tau_{\mathrm{WB}} \gg \tau_m$, which can be estimated by requiring that $|\partial_x E_x| = 4\pi e n_0$. Assuming a short laser driver with duration $\tau_L \sim 1/\omega_p$ and the nonrelativistic normalized vector potential $|\mathbf{a}^2| \ll 1$, we estimate that $\tau_{\mathrm{WB}} \approx 2\tau_m / |\mathbf{a}^2|$.

VIII. CONCLUSIONS

In summary, an analytic theory of laser wake excitation in an arbitrary plasma channel is developed. Although plasma channels with smooth monotonic density profiles do not support any true eigenmodes, the damped quasi-modes have been formally derived using the Laplace transform and the method of analytic continuation. A numerical procedure for computing the frequencies and the damping rates of such quasi-modes is developed. Excellent agreement of these numerical results and the explicit fluid simulation is found over a wide range of parameters. For wide plasma channels analytical results, predicting the algebraic decay of the wake field with time, are obtained. Wake fields decay because of the phase-mixing of the plasma currents at different transverse locations inside the channel. Physical interpretation of this phase-mixing, based on the nonlocal nature of the electromagnetic wakes, is presented.

ACKNOWLEDGMENTS

The authors acknowledge useful conversations with N. J. Fisch, B. A. Shadwick, and J. S. Wurtele.

This work was supported by the U.S. Department of Energy, Division of High Energy Physics.

[1] T. Tajima and J. M. Dawson, Phys. Rev. Lett. **43**, 267 (1979).
[2] L. M. Gorbunov and V. I. Kirsanov, Zh. Exp. Teor. Fiz. **93**, 509 (1987) [Sov. Phys. JETP **66**, 290 (1987)].
[3] C. Joshi, W. B. Mori, T. Katsouleas *et al.*, Nature (London) **311**, 525 (1984).
[4] P. Sprangle, E. Esarey, A. Ting, and G. Joyce, Appl. Phys. Lett. **53**, 2146 (1988).
[5] J. S. Wurtele, Phys. Fluids B **5**, 2363 (1993); Phys. Today **47** (7), 33 (1994), and references therein.
[6] P. Sprangle and E. Esarey, Phys. Fluids B **4**, 2241 (1992).
[7] E. Esarey, P. Sprangle, J. Krall, A. Ting, and G. Joyce, Phys. Fluids B **5**, 2578 (1993).
[8] C. E. Clayton, K. A. Marsh, A. Dyson, M. Everett, A. Lal, W. P. Leemans, R. Williams, and C. Joshi, Phys. Rev. Lett. **70**, 37 (1993).
[9] S. Suckewer and C. H. Skinner, Science **247**, 1553 (1990), and references therein.
[10] H. M. Milchberg, C. G. Durfee III, and J. Lynch, J. Opt. Soc. Am. B **12**, 731 (1994).
[11] H. M. Milchberg, C. G. Durfee III, and T. J. McIlrath, Phys. Rev. Lett. **75**, 2494 (1995).
[12] M. Tabak, J. Hammer, M. E. Glinsky, W. L. Kruer, S. C. Wilks, J. Woodworth, E. M. Campbell, M. D. Perry, and R. J. Mason, Phys. Plasmas **1**, 1626 (1994).
[13] C. G. Durfee III and H. M. Milchberg, Phys. Rev. Lett. **71**, 2409 (1993); C. G. Durfee III, J. Lynch, and H. M. Milchberg, Phys. Rev. E **51**, 2368 (1995).
[14] Y. Ehrlich, C. Cohen, A. Zigler, J. Krall, P. Sprangle, and E. Esarey, Phys. Rev. Lett. **77**, 4186 (1996); A. Zigler, Y. Ehrlich, C. Cohen, J. Krall, and P. Sprangle, J. Opt. Soc. Am. B **13**, 68 (1996).
[15] V. L. Ginsburg, *Propagation of Electromagnetic Waves in Plasma* (Addison–Wesley, Reading, 1964).
[16] J. P. Freidberg, R. W. Mitchell, R. L. Morse, and L. I. Rudsinski, Phys. Rev. Lett. **28**, 795 (1972).
[17] W. L. Kruer, *The Physics of Laser Plasma Interactions* (Addison–Wesley, Reading, 1988), and references therein.
[18] K. R. Stepanov, Sov. Phys. Tech. Phys. **10**, 773 (1965).
[19] Z. Sedláček, J. Plasma Phys. **5**, 239 (1971); **6**, 187 (1971).
[20] T. Katsouleas, T. C. Chiou, C. Decker, W. B. Mori, J. S. Wurtele, G. Shvets, and J. J. Su, AIP Conf. Proc. **279**, 480 (1993).
[21] T. C. Chiou, T. Katsouleas, C. Decker, W. B. Mori, J. S. Wurtele, G. Shvets, and J. J. Su, Phys. Plasmas **2**, 310 (1995).
[22] G. Shvets and J. S. Wurtele, AIP Conf. Proc. **351**, 24 (American Institute of Physics, Woodbury, NY, 1996).
[23] G. Shvets, J. S. Wurtele, T. C. Chiou, and T. Katsouleas, IEEE Trans. Plasma Sci. **24**, 351 (1996).
[24] W. Leemans, C. W. Siders, E. Esarey, G. Shvets, N. Andreev, and W. B. Mori, IEEE Trans. Plasma Sci. **24**, 331 (1996).
[25] N. E. Andreev, L. M. Gorbunov, V. I. Kirsanov, K. Nakajima, and A. Ogata, Phys. Plasmas **4**, 1145 (1997).
[26] L. D. Landau, J. Phys. (Moscow) **10**, 25 (1946).
[27] L. A. Dikii, Dokl. Acad. Nauk. SSSR **135**, 1068 (1960) [Sov. Phys.-Dokl. **5**, 1179 (1960)]; C. C. Lin, *The Theory of Hydrodynamic Stability* (Cambridge University Press, London, 1955).
[28] R. J. Briggs, J. D. Daugherty, and R. H. Levy, Phys. Fluids **13**, 421 (1970).
[29] N. R. Corngold, Phys. Plasmas **2**, 620 (1995).
[30] G. Shvets and J. S. Wurtele, Phys. Rev. Lett. **73**, 3540 (1994).
[31] P. Sprangle, J. Krall, and E. Esarey, Phys. Rev. Lett. **73**, 3544 (1994).
[32] L. Gorbunov, P. Mora, and T. M. Antonsen, Jr., Phys. Rev. Lett. **76**, 2495 (1996).
[33] J. W. S. Rayleigh, Proc. London Math. Soc. **11**, 57 (1880).
[34] W. Kelvin, Nature (London) **23**, 45 (1880).
[35] In principle, the defining equation $\omega_p^2(x_r) = \omega^2$ can have multiple roots $x_r^{(j)}$. We will be referring as x_r to a root which crosses the real x-axis for $\omega_i = 0$.
[36] B. A. Shadwick and J. S. Wurtele, in *Proceedings of the Sixth European Particle Accelerator Conference*, Stockholm, 1998, edited by S. Myers, L. Liljeby, Ch. Petit-Jean-Genaz, J. Poole, and K.-G. Rensfelt (Institute of Physics Publishing, Philadelphia, 1998), p. 827.
[37] Carl M. Bender and Steven A. Orszag, *Advanced Mathematical Methods For Scientists And Engineers* (McGraw–Hill, New York, 1978).
[38] W. Magnus, F. Oberhettinger, and R. P. Soni, *Formulas and Theorems for the Special Functions of Mathematical Physics*, 3rd ed. (Springer, Berlin, 1966).
[39] J. M. Dawson, Phys. Rev. **113**, 383 (1959).
[40] S. V. Bulanov, F. Pegoraro, A. M. Pukhov, and A. S. Sakharov, Phys. Rev. Lett. **78**, 4205 (1997).